Science of the Total Environment 699 (2020) 134244

Contents lists available at ScienceDirect

Science of the Total Environment

journal homepage: www.elsevier.com/locate/scitotenv

Temporal evolution characteristics of PM2.5 concentration based on continuous wavelet transform

Xiaobing Chen [a], Lirong Yin [b], Yulin Fan [c], Lihong Song [a], Tingting Ji [a], Yan Liu [a], Jiawei Tian [a], Wenfeng Zheng [a,*]

[a] School of Automation, University of Electronic Science and Technology of China, Chengdu 610054, Sichuan, PR China
[b] Geographical and Sustainability Sciences Department, University of Iowa, Iowa City, IA 52242, USA
[c] School of Foreign Languages, Sichuan Normal University, Chengdu 610101, PR China

HIGHLIGHTS

- The evolutionary characteristics of PM2.5 vary with time.
- Wavelet transform is powerful to capture the temporal features of PM2.5 concentration at different scales.
- In the temporal characteristics of PM2.5 from 2014 to 2017, there exist multiple oscillation periods.
- The time scale of 216-389 d is the predominant oscillation period of the PM2.5 daily evolution.
- In the evolution of PM2.5 in 120 hours, the dominant period experiences two abrupt changes.

GRAPHICAL ABSTRACT

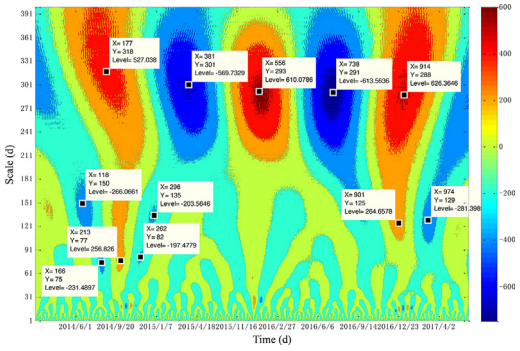

ARTICLE INFO

Article history:
Received 23 April 2019
Received in revised form 12 August 2019
Accepted 1 September 2019
Available online 2 September 2019

Editor: Pavlos Kassomenos

ABSTRACT

Fine particulate matter (PM2.5) is an important haze index, and the researches on the evolutionary characteristics of the PM2.5 concentration will provide a fundamental and guiding prerequisite for the haze prediction. However, the past researchers were usually based on the overall time-domain evolution information of PM2.5. Since the temporal evolution of PM2.5 concentration is nonstationary, previous studies might neglect some important localization features that the evolution has various predominant periods at different scales. Therefore, we applied the wavelet transform to study the localized intermittent oscillations of PM2.5. First, we analyze the daily average PM2.5 concentration collected from the automatic monitoring stations. The result reveals that the predominant oscillation period does vary with time. There exist multiple oscillation periods on the scale of 14–32 d, 62–104 d, 105–178 d and 216–389 d and the 298d is the first dominant period in the entire evolutionary process. Moreover, we want to figure out whether the temporal characteristics of PM2.5 in the days with heavy haze also have localized intermittent periodicities. We select the hourly average PM2.5 concentration in 120 h when the haze pollution is serious. We find that the principal period has experienced two abrupt shifts and the energy at the 63-hour scale is the most powerful. The results in these two independent analyses come into the same conclusion that the multiscale features shown in the temporal evolution of PM2.5 cannot be ignored and may play an important role in the further haze prediction.

© 2019 Elsevier B.V. All rights reserved.

* Corresponding author.
E-mail address: wenfeng.zheng.cn@gmail.comPlease confirm that the provided email wenfeng.zheng.cn@gmail.com is the correct address for official communication, else provide an alternate e-mail address to replace the existing one, because private e-mail addresses should not be used in articles as the address for communication. (W. Zheng).

https://doi.org/10.1016/j.scitotenv.2019.134244
0048-9697/© 2019 Elsevier B.V. All rights reserved.

1. Introduction

Many countries have been suffering from the haze pollution, including China, the United States, Britain, Germany, Japan and France. Haze pollution has become an important threat to the global environment (Schichtel et al., 2001; Vautard et al., 2009; Neiburger and Wurtele, 1949; Doyle and Dorling, 2002). From January 2013, China has suffered from severe haze pollution for the first time in a large scale. The Air Quality Index in some areas exceeded 500 (Wang et al., 2014). Since the late 2016, the problem of haze pollution has spread from only some regions to all parts of the country covering 25 provinces and the situation has become fiercer. More than 100 large and medium-sized cities have haze pollution in different levels, which not only affects the traffic condition, but also causes direct harm to people's physical and mental health.

In the first stage of researches on the haze, researchers focused on the chemical composition, causing factors (Hu et al., 2006; Lonati et al., 2005) and pollution detection (Gupta et al., 2007; Thurston et al., 2011; Chen et al., 2017; Okamoto et al., 1990). As more and more meteorological stations have been built and the observational data related to the pollutants are available, the prediction of haze has been a heat spot. Many researchers have focused on establishing different haze prediction models. GW Fuller et al. (2002) designed an empirical model to predict the daily average concentrations of PM2.5 and PM10 in London. Jian et al. (2012) used the Autoregressive Integrated Moving Average (ARIMA) to predict the PM10 concentration in busy traffic areas in Hangzhou. Dong et al. (2009) proposed a hidden Markov model based on predicting high PM2.5 concentrations in haze-contaminated weather. C Chemel (Xi-Qin et al., 2018) established the chemical conversion model CMAQ to model PM2.5 concentration data in the UK and predicted changes in the annual average PM2.5 concentration.

Besides a good model, the studies on the temporal evolution characteristics of haze are needed for further haze prediction. The temporal characteristics of the haze, such as periodicity, can exhibit the macroscopic characteristics of haze evolution and can serve as a time domain partitioning criterion to support the haze prediction model. Thus, some researchers analyzed the temporal characteristics of PM2.5 or PM10 concentrations by collecting the hourly and daily data from various observation stations. Rodríguez et al. (2003) used meteorological data and satellite observations of African dust plumes to analyze the spatial and temporal variations of PM levels from 1996 to 2000 in Northeastern Spain and found that the maximum PM levels were varied with the difference of districts. Zhang et al. (2015) collected the hourly and daily records of PM2.5 and O3 from two stations in Beijing, the capital of China, to examine the long-term trends of evolution of PM2.5 and O3 concentrations and the certain links between the variability of pollutant concentrations and meteorological variables on the synoptic time scale. Song et al. (2015) defined a concept named PM2.5 Pollution Episodes (PPEs) to represent the period with serious haze and they collected the hourly PM2.5 concentration observations in Beijing to analyze the evolution mode of each PPE. They found that the PPEs showed significant seasonal variations that the most serious haze occurred in winter while the PPEs with long duration occurred in autumn. Hu et al. (2013) also used the PM10 concentration from 27 stations in Beijing to explore the spatial and temporal characteristics of PM10, and the result demonstrated the variation of PM10 concentration in different seasons and stations.

Although there are a lot of efforts put on the temporal characteristics of PM2.5/PM10 concentration, almost all the researches are based on a simple method that the temporal characteristics of PM2.5/PM10 is evaluated with the assumption that statistical properties of the time series do not vary with time. However, in reality, the evolution of PM2.5 is nonstationary. This is to say, the dominant modes of the variability will vary with time. Meteorological dynamics can switch between different dynamics at different scales, influenced by complicate factors, including the geographical features and seasons etc. Figuring out the fine-grained temporal characteristics will aid researchers to build more sophisticated haze prediction models and help to reveal more details of pollutant evolution.

Therefore, in this paper, we study on the Chengdu city, an area with severe haze in China. The daily average PM2.5 concentration data as the haze index from June 2014 to June 2017 are analyzed to reveal the localized intermittent oscillations in the unit of day. We use the continuous wavelet transform (CWT) that is good at capturing the localization features of nonstationary sequence. The Morlet complex wavelet is selected as the mother wavelet to perform time-scale transformation on the original sequence and obtain complex wavelet coefficients. Based on the complex wavelet coefficients, the modulus and the real part of coefficients are used to reveal the oscillation period of PM2.5.

In addition, we also care about the evolutionary features of PM2.5 in the days with heavy haze, which may provide the essential haze forecast to prepare people for the incoming serious haze. Therefore, we collected 120 observations of hourly PM2.5 concentration in the period with heavy haze and applied the same method used in the analysis of the daily data.

2. Data and methods

2.1. Dataset

Chengdu (30.67°N, 104.06°E), the largest city in southwestern China with about 11 million residents and an area over 12,000 km^2, is sited at the western part of the Sichuan Basin and surrounded by Longquan Mountain to the east and Qionglai Mountain to the west of the it (Fig. 1a). Due to the special geographical position, it is one of the cities with most serious air pollution, especially PM concentration. Besides the location, the meteorological condition also deteriorates the air condition. The wind direction rarely changes and the annual average wind speed is 1.2 m/s, with high static wind frequency, up to 45%–50%. (Yin et al., 2013) Thus, the pollution situation is almost stable and thus suitable for us to study the variation of PM2.5 concentration at multiple time scales.

For exploring the variation of PM2.5 concentration, we collected PM2.5 concentration data from the China Air Quality Online Monitoring and Analysis Platform (www.aqistudy.cn/). There are six automatic monitoring stations (Fig. 1b), Sanwayao, Caotangsi, Junpingjie, Liangjiahe, Shahepu, Shilidian in Chengdu. We got 1050 daily average PM2.5 concentration readings ranging from June 2014 to June 2017 from each station, and the missing data have been replaced by the mean of two nearest data. In this paper, we focused on the holistic pollution conditions in Chengdu, so we calculated the mean of data from six monitoring stations as the daily average PM2.5 concentration. Eventually we gained 1073 entries for daily PM2.5 concentration.

The daily average PM2.5 concentration (Fig. 2) includes the readings from June 2014 to June 2017. Obviously, the variation of PM2.5 concentration is dominated by the annual cycle, but the inner variation has connection with the period, which means there are different periodic features at the view of various timescales. The top three PM2.5 concentration occurred in January 15, 2015, when PM2.5 concentration is 238 $\mu g/m^3$, December 30, 2015, when PM2.5 concentration is 255 $\mu g/m^3$, and December 26, 2016,

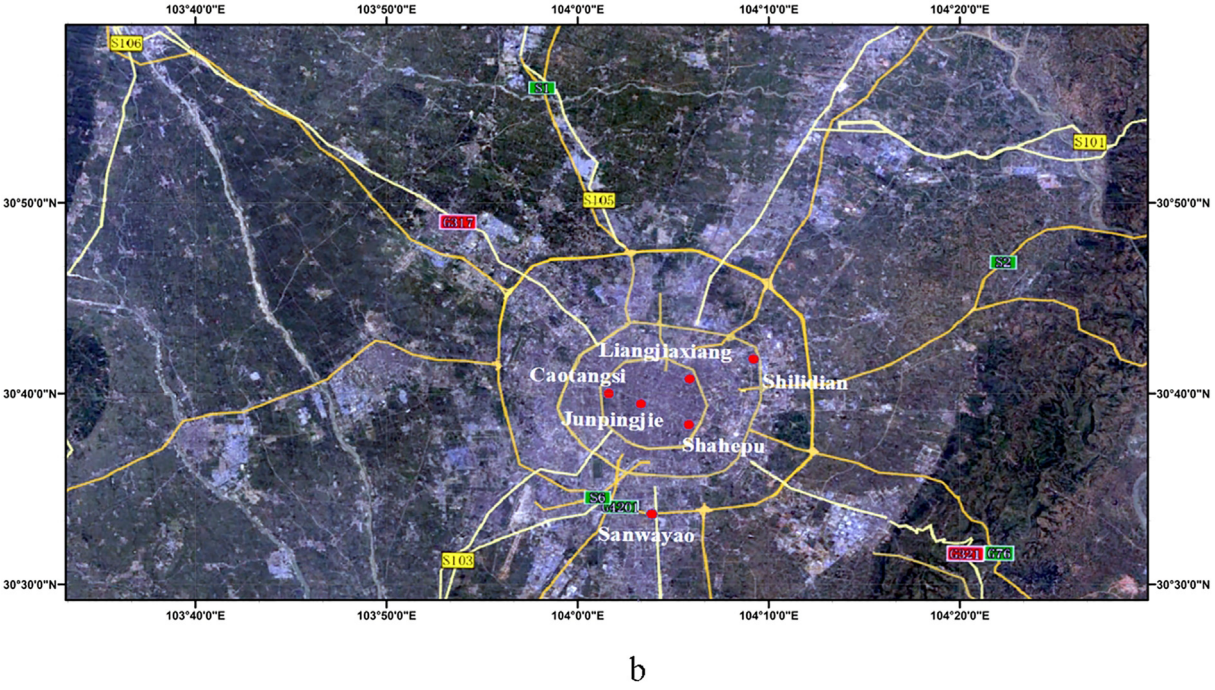

Fig. 1. a is the topography of the Sichuan Basin; b is the distribution of the six monitoring stations in Chengdu.

when PM2.5 concentration is 280 μg/m^3. Chengdu has 299 days per a year with air pollution that include 3 serious ones and 54 high-haze days (Table 1).

According to the daily PM2.5 concentration, the January in 2016, one of the periods with heavy haze, is suitable to study the localized intermittent periodicities of PM2.5 in the serious haze days. We collected 120 hourly PM2.5 concentration data during 0:00 on 2nd January to 23:00 on January 6, 2016. The specific details about the hourly data will be informed in the Section 3.2.1.

2.2. Wavelet analysis

Wavelet analysis is a powerful tool to study localized variations of power within a time series. It will be helpful to reveal both the dominant modes of variability and how those modes vary in time after decomposing a time series into time–frequency space (Torrence and Compo, 1998). Since the wavelet analysis was applied in the analysis of seismic signals (Morlet et al., 1982), it has been widely used in scientific, engineering, mathematic com-

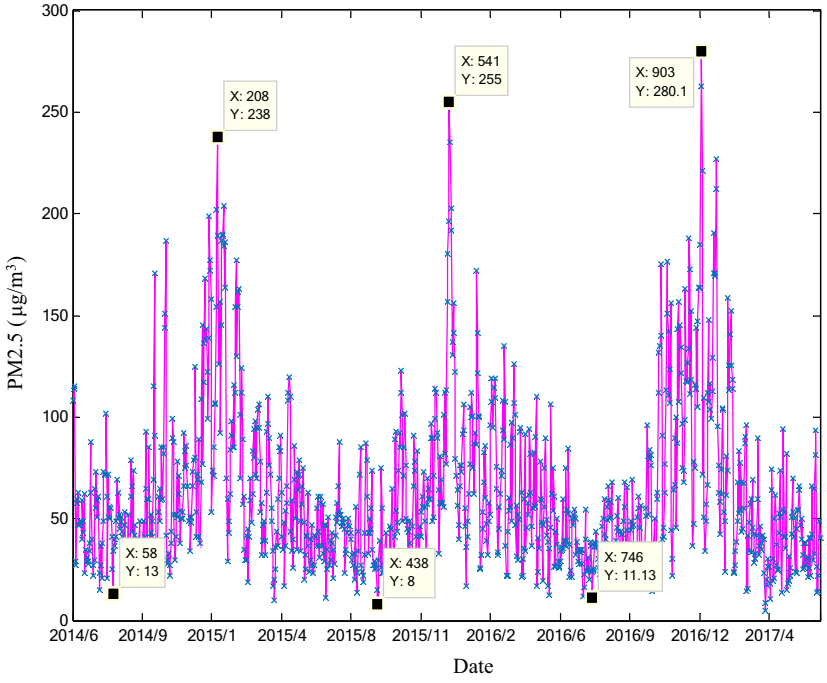

Fig. 2. The daily average PM2.5 concentration in Chengdu from June 2014 to June 2017.

Table 1
Haze pollution in Chengdu from 2014 to 2017.

Level	Serious DC ≥ 250	High 250 ≥ DC ≥ 150	Moderate 150 ≥ DC ≥ 115	Low 115 ≥ DC ≥ 75
N	3	54	52	190

DC denotes Daily PM2.5 Concentration in the unit of μg/m^3.
N denotes the number of days.

munity with its versatile applicability, especially in the geophysics (Weng and Lau, 1994; Baliunas et al., 1997; Zheng et al., 2017). Compared to the Fourier transform, wavelet analysis can better deal with signals that contain nonstationary power at many different frequencies (Daubechies, 1990). The wavelets obtained by scaling and translating the *wavelet function* not only fits the region of sharp change in the signal that are nonstationary, but also extracts the local characteristic of the signal, and obtains the periodic variation under the specific scale. Because of the time-frequency localization property of the wavelets, wavelets are apt to time-frequency and time-scale analysis. The variation of PM2.5 concentration is the kind of data with different frequencies at various scales, thus applying the wavelet transform on the PM2.5 data is a good way to trace its evolution in time series.

The wavelet transform has two transform methods: continuous wavelet transform (CWT) and discrete wavelet transform (DWT). Discrete wavelet transform is suitable for data compression and signal denoising processing (Grinsted and Moore, 2004). Continuous wavelet transform is better at extracting signal features, so it is widely used to extract intermittent wave characteristic of time series in geophysical research (Adrianac et al., 2008). In this paper, only the continuous wavelet transform (CWT) is selected to study the temporal characteristics of PM2.5.

We have the time series of the PM2.5 concentration, x_n, with equal time spacing δt and $n = 0 \ldots N-1$. And we also have the *mother wavelet* $\psi(t)$, which depends on a non-dimensional "time" parameter t. For satisfying the admissibility conditions, where $\psi(w)|_{w=0} = 0$ and $\psi(t)$ must have zero mean and be located in the both time and frequency space (Farge, 1992):

$$C_\psi = \int_{-\infty}^{+\infty} \frac{|\psi(w)|^2}{|w|} dw < \infty \quad (1)$$

The continuous wavelet transform of the discrete sequence x_n is defined as the convolution of x_n with the daughter wavelets which are the translated and scaled versions of the mother wavelet $\psi(t)$:

$$W_n^X(s) = \sqrt{\frac{t}{s}} \sum_{n'=0}^{N-1} x_{n'} \psi * \left(\frac{(n'-n)t}{s} \right) \quad (2)$$

where the (*) indicates the complex conjugate. The $W_n^X(s)$ is also named wavelet coefficient, which indicates the correlation between the wavelet (at a certain scale) and the data array (at a particular location). The *wavelet scale s* and the *localized time index n* are continuous real numbers, $s \in R^+$, $n \in R$. The larger the *wavelet scale s*, the wider the $\psi(t/s)$, and the signal characteristics are more apparent in the multi-scale of the original signal. The *localized time index n* controls the translation transform of the mother wavelet. By changing the *wavelet scale s* and translating along the *localized time index n*, one can construct a picture showing both the amplitude of any features versus the scale and how this amplitude varies with time.

The *wavelet power spectrum* is defined as $|W_n^X(s)|^2$, which indicates the wave magnitude in the specified wavelet scale and time domain (Flandrin, 1992). If the Morlet wavelet is selected as the mother wavelet, the imaginary part of the wavelet coefficients can be interpreted as the local phase.

The *wavelet variance Var(s)* is the integral of the squared norm of the wavelet coefficients in the time domain, which indicates the periodic wave energy distribution under the different scales. When the scale is fixed, the greater the wavelet variance is, the

greater the intensity of the oscillation is, and the more obvious the periodic characteristics are, which means that the time series signal has the main period. The wavelet variance is as shown in formula (3).

$$\mathrm{Var}(s) = \int_{-\infty}^{+\infty} W_n^X(s)^2 dn \tag{3}$$

2.2.1. Choice of the mother wavelet

The different types of mother wavelet have the different influence on the signal transformation. In orthogonal wavelet analysis, the number of convolutions at each scale is related with the width of the mother wavelet at the same scale. In the wavelet power spectrum, there are discrete parts of wavelet power which is beneficial for signal processing because it has the most compact representation of the signal. However, it is not good enough for time series analysis. A nonorthogonal analysis is highly redundant at large scales, so the representation at adjacent times in the wavelet spectrum is highly correlated. The nonorthogonal transform is useful for time series analysis, where smooth, continuous variations in amplitude are needed (Abry and Veitch, 1998).

Choosing real wavelet or complex one also has different effects. Using a complex wavelet function will yield information about both amplitude and phase, so it is better adapted for capturing oscillatory behavior. In contrary, only a single component can be gained by applying a real wavelet function, so it can be used to isolate peaks or discontinuities.

In the paper, to simultaneously preserve the amplitude and phase information of the sequence signal of PM2.5 concentration, we select the *Morlet wavelet* as the mother wavelet, which is a single frequency complex sinusoidal function and has the symmetry and the non-orthogonality and the imaginary part, which can express the phase information well, as shown in formula (4).

$$\psi_0(t) = (\pi \times f_b)^{-1/2} e^{2i \times fc \times t} e^{-t^2/f_b} \tag{4}$$

In (4), t represents time and f_b represents bandwidth controlling the attenuation in the time domain and the corresponding bandwidth in the frequency domain. f_b is the reciprocal of variance in the frequency domain. The increase of f_b will make the wavelet energy concentrated around the center frequency and slow down the attenuation speed in the time domain. Reversely, the reduction of f_b will accelerate the decay rate in the time domain and reduce the energy of the frequency domain. f_c denotes the center frequency and affects the frequency value when the time domain is converted to the frequency domain. ψ(t) is a complex Morlet wavelet determined by f_b and f_c. In this paper, we set the f_b to be 1.5 and the f_c to be 1, shown in the Fig. 3.

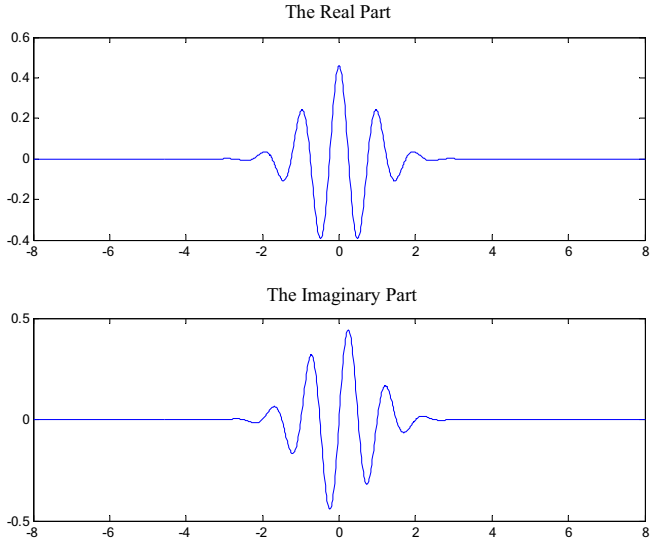

Fig. 3. The real and imaginary parts of the Morlet wavelet with f_b = 1.5 and f_c = 1.

3. Temporal evolution characteristics of PM2.5 based on CWT

PM2.5 is an important variable in the study of haze pollution, and there exist localized intermittent oscillations in the evolution of PM2.5, which means that there is no consistent period in the process, and the period of PM2.5 evolution varies at different wavelet scales.

Compared with past researches on the evolution of PM2.5 concentration of which most neglect that the PM2.5 evolution is nonstationary in time, we apply the wavelet transform to the study of the periodic characteristics. Specifically speaking, we apply the same method to the two distinct circumstances that will benefit the different haze prediction models. One is the analysis of the daily average PM2.5 concentration in three years that will yield localized intermittent oscillations in the unit of day and is especially useful for the haze prediction in a year, and the other is on the hourly PM2.5 concentration in five days when there is serious haze, which is meant to reveal the evolutionary features of PM2.5 in the period with heavy haze when air quality is more concerned by individuals.

3.1. Temporal characteristics of PM2.5 in three years

3.1.1. Data preprocessing and parameter setting

As illustrated in the Section 2.1, we collected the daily average PM2.5 concentration from six monitoring stations, Sanwayao, Caotangsi, Junpingjie, Liangjiaxiang, Shahepu, Shilidian. The readings are from June 2014 to 2017 and the number of entries is 1073. Before the data does the convolution with the wavelet mother ψ (t), we applied data preprocessing to reduce the errors that will occur at the beginning and end of the wavelet power spectrum since the sequence of PM2.5 concentration is finite-length. We padded 63 and 64 zeros respectively to the head and the tail of the sequence (Meyers et al., 1993), so the length of data extends to 1200. After the wavelet transform, the added data are removed to ensure the authenticity of data.

In the aspect of parameter setting, the time series data x_n has the equal time spacing $\delta t = 1$ *(d)* and $N = 1072$. While deciding the *wavelet scale s*, we followed two expressions:

$$s_j = s_0 2^{ij}, j = 0, 1, J \tag{5}$$

$$\mathrm{J} = \sigma j^{-1} \log_2(Nt/s_0) \tag{6}$$

where s_0 is the smallest resolvable scale and J determines the largest scale. For the Morlet wavelet, the σj can be set to 0.5. Here we set s_0 to be 2, and J to be 16, giving scales from 2 d up to 512 d.

The f_b and f_c of the *Morlet wavelet* are set to be 1.5 and 1 respectively. Because of the parameter settings of the Morlet wavelet in our paper, the wavelet scale is almost equal to the Fourier period. Thus, we directly use the wavelet scale in following analysis.

3.1.2. Result

According to the convolution (2), 1200 entries of our daily average PM2.5 concentration are calculated to produce *the wavelet coefficient* $W_n^X(s)$. After the wavelet transform, we removed the first 63 columns and the last 64 columns that were added in the data preprocessing. Eventually, we obtained a $400 * 1073$ wavelet coefficient matrix of the daily average PM2.5 concentration. Furthermore, we depicted the real part of wavelet coefficients $R\{W_n^X(s)\}$

that could show the power distribution in the different time and scale, modulus of the wavelet transform $|W_n^X(s)|$ that could reveal energy density distribution on different scales, and the wavelet variance *Var(s)* that is beneficial to show the fluctuation conditions of PM2.5 daily concentration telling which is the main period and the change pattern of the periods within a certain time span.

The real part of wavelet coefficients $R\{W_n^X(s)\}$ is a powerful tool to study the energy distribution of the PM2.5 concentration over time, frequency, and scale, as shown in Fig. 4, where the horizontal axis represents time in the unit of day and the vertical axis represents the wavelet scale. Obviously, there exist distinct scales of variation of the PM2.5 concentration in the entire time domain, which can provide us with an overall cognition of the variation trend to predict the further changes. If the region of the contour map is filled with the warm color, the real part is positive which means that the air quality of Chengdu city is poor, and the haze pollution is serious. If the filling color is cold, the real part is negative, indicating that the air quality in Chengdu is good, and haze pollution does not exist or is slight.

Fig. 4 shows that there are multiple periods of the daily average PM2.5 concentration from June 2014 to June 2017, which are on the scale of 14–32 d, 62–104 d, 105–178 d and 216–389 d. In particular, there are obvious oscillations on the scale of 216–389 d, and the periodic characteristics are very stable, covering the time domain. There is a dominant oscillatory period of 279–368 d in the evolution of daily PM2.5 concentration, which is the convergence of several small oscillation periods. In the entire time domain, there are three warm centers in December 2014, January 2016 and January 2017 respectively, during the winter, the period with serious haze pollution; two cold centers occur on July 2015 and July 2016, corresponding to the annual summer, when haze pollution does not exist or is slight. This is, the energy distribution shown in the Fig. 4 reveals a good conformity with the realistic conditions.

The modulus of the wavelet transform $|W_n^X(s)|$ (Fig. 5) shows that the principal oscillation period varies with time, even though the energy tends to gather in the 270–370-day band. The periodic vibration energy on the scale of 270–370 d is the strongest, and the period is relatively significant, and the periodic change is through the entire domain; the periodic vibration energy on the scale of 140–230 d is weak, which is localized; the periodic vibration energy on the scale of 0–140 d is very weak, occupying the time domain.

The greater the modulus of the wavelet coefficients is, the more apparent the periodicity at the corresponding scale is. It can be clearly seen that during the evolution of the daily PM2.5 concentration, the dominant oscillation period decreases with the time, though there exists no sudden change in prominent frequency. In the first 400 days, the principle oscillation is around 325d, and it shifts to about 300d after 500th d. The oscillation period becomes more stable in the evolution process, and it demonstrates that there are no dramatic period changes in the PM2.5 concentration.

The oscillation amplitude of PM2.5 concentration has the relatively obvious changes during the 1073 days. The overall evolution trend of the energy is increasing, that the powerless periods is during first 500 days and the energy after the 500th d have experienced an apparent increase.

To examine the amplitude modulation, we plotted the variance of wavelet coefficient of daily PM2.5 concentration (Fig. 6), which describes the fluctuation distribution of PM2.5 concentration sequence at different scales. The value of the variance shows the power of the fluctuation, this is, the bigger the variance is, the more dominant the oscillation at this scale is. Therefore, we can obtain the dominant period from the variance diagram. There is one apparent peak in Fig. 6, which corresponds to the scale of 298d and means that the periodic oscillation is the strongest at this scale. So, the scale of 298d is the first dominant period indicating that the fluctuation of the period almost controls the fluctuant

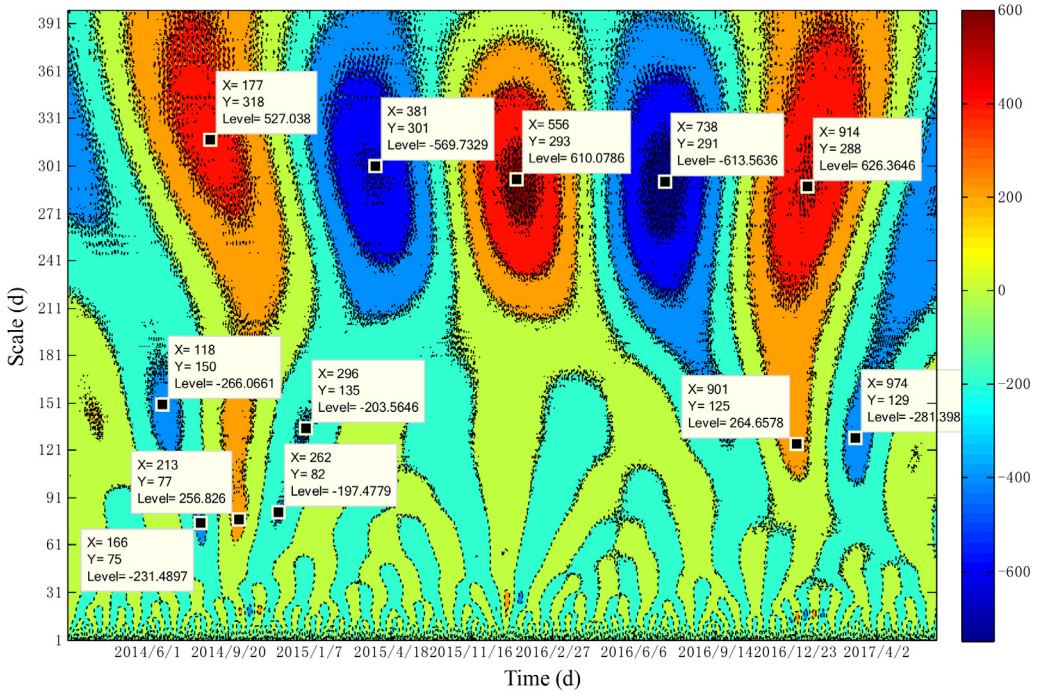

Fig. 4. The real part of wavelet coefficients $R\{W_n^X(s)\}$ in three years. The horizontal axis represents time in the unit of day and the vertical axis represents the scale in the unit of day.

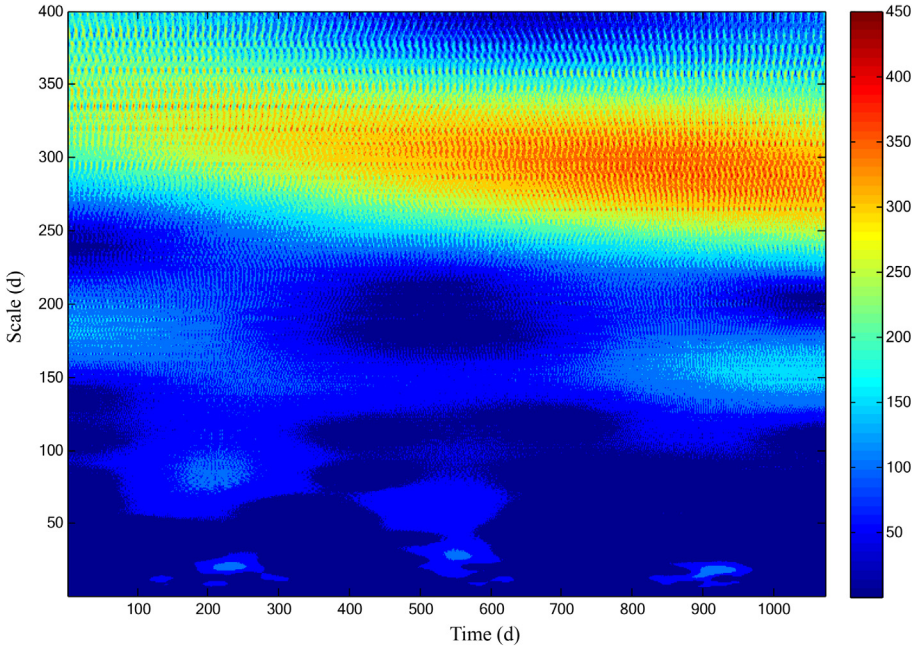

Fig. 5. The modulus of the wavelet transform $|W_n^X(s)|$.

characteristics of the daily average concentration in the entire time domain.

We plotted the real part of wavelet coefficients (Fig. 7) on the scale of 298d, the principal period. The plot shows that three up-down conversion happened in the three years.

3.2. Temporal characteristics of PM2.5 in 120 h

As shown in the Fig. 4, the warm regions are mostly distributed in the winter, especially in December 2014, January 2016 and January 2017 when the haze pollution were most serious. From the above analysis, we found the dominant oscillation within three years and the average period of PM2.5 concentration, which would provide forward-looking data foundation for the haze prediction in a year. But, in reality, individuals may concern more about the real-time haze forecast, especially during the period with the heavy haze.

Therefore, knowing the meaning of localized intermittent periodicities of PM2.5 in the days with serious haze is significant. We employed the same wavelet transform to the analysis for the purpose of finding whether there are distinct oscillations in the period with heavy haze.

3.2.1. Dataset and parameter setting

Since the January in 2016 is one of the periods with heavy haze, we collected the hourly PM2.5 concentration from the six automatic monitoring stations in Chengdu during 0:00 on 2nd January to 23:00 on January 6, 2016.

In order to avoid the boundary effect, we also padded 15 zeroes in the start and end of the time sequence expanding the total number of entries to 150. The complex Morlet wavelet was selected as the mother wavelet, the max scale was 64 h, the bandwidth was set to 1.5, the center frequency was set to 1. After eliminating the first 15 columns and the last 15 columns, we got a $64 * 120$ complex wavelet coefficient matrix preparing for the further discussion.

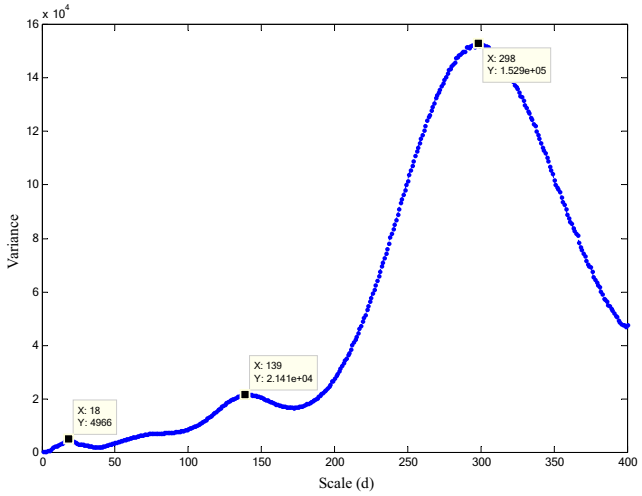

Fig. 6. The variance of wavelet coefficient of daily PM2.5 concentration.

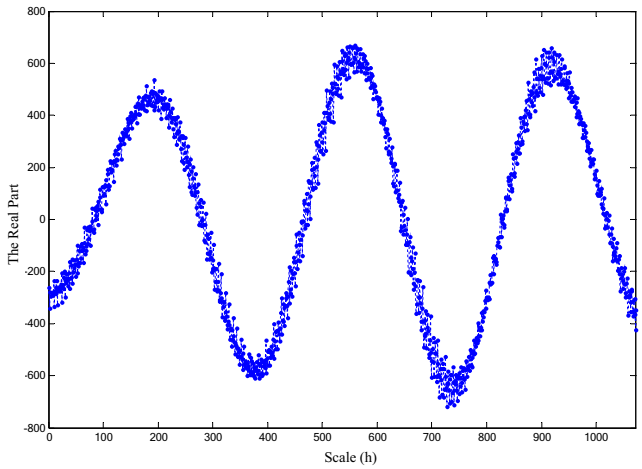

Fig. 7. The real part of wavelet coefficients at the 298d scale.

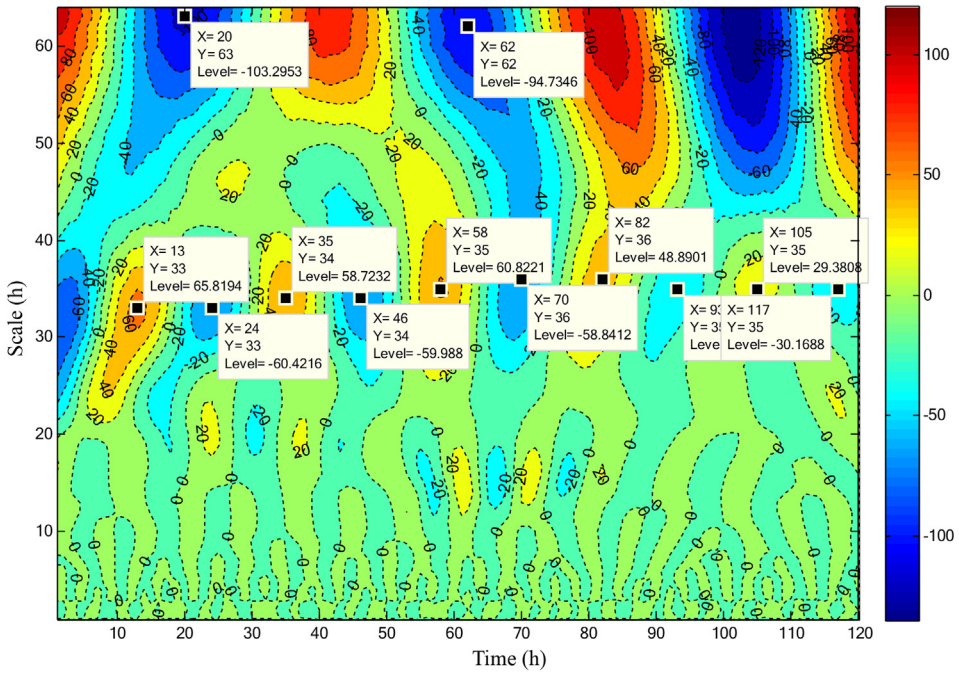

Fig. 8. The Real Part of Wavelet Coefficients $R\{W_n^X(s)\}$ in 120 h. The x axis indicates the time and the y axis represents the scale with the same unit of hour.

3.2.2. Result

The real part of wavelet coefficients $R\{W_n^X(s)\}$ in 120 h is shown in Fig. 8. There are three apparent periodic changes during the evolution of PM2.5 concentration, on the scale of 12–22 h, 23–42 h and 45–64 h. Especially on the scale of 23–42, there are five oscillating processes, and the periodic characteristics are very stable in the whole time domain. The warm centers are distributed in the time of 2nd h, 45th h 85th h and 120th h at about forty-hourly intervals, and the cold centers are in the time of 22nd h, 65th h, 105th h at about forty-hourly intervals.

The modulus of the wavelet transform $|W_n^X(s)|$ (Fig. 9) shows the corresponding energy density distribution in the time domain on different scales. The energy patterns reveal that there exist obvious predominant oscillation changes. The PM2.5 concentration is characterized by a strong 62-h oscillation during the first 20 h. At the 20th h, the predominant period suddenly changes from 62 h to 34 h, and it continues to the 80th h. And after the 80th h, the principal period increases to 64 h gradually. The energy amplitude of the PM2.5 concentration also follows the similar pattern as the change of the main oscillation. The first 20 h and the last 40 h

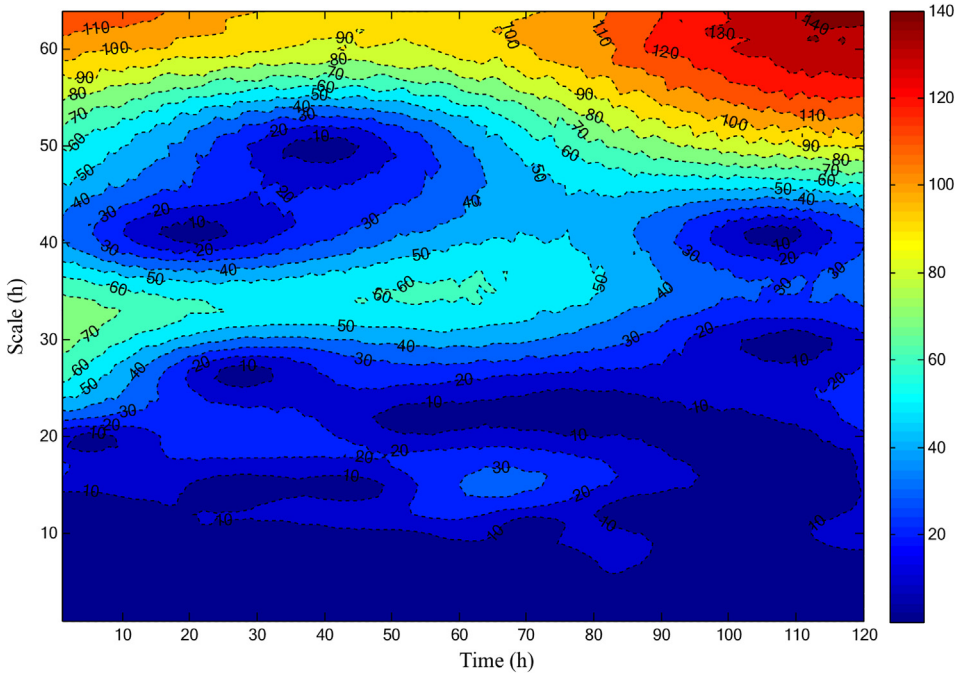

Fig. 9. The modulus of the wavelet transform $|W_n^X(s)|$ in 120 h.

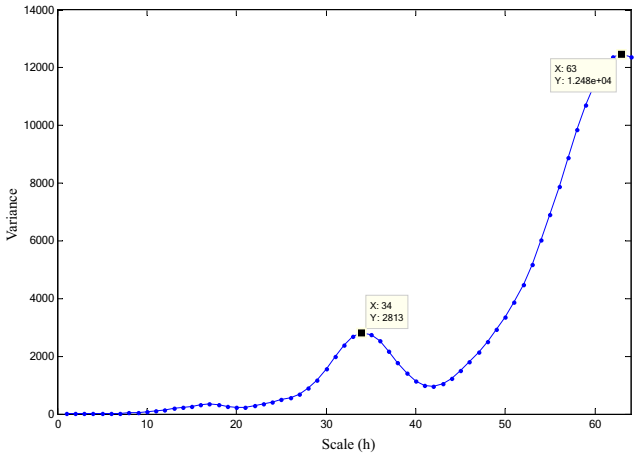

Fig. 10. The variance of wavelet coefficient of hourly PM2.5 concentration.

are the powerful periods, and the powerless period is during the 20th h to 80th h.

The variance of wavelet coefficient of hourly PM2.5 concentration (Fig. 10) is also plotted to study the fluctuation of PM2.5 at the various scales. The variance changes as we discussed above, that there are two peaks occurring in the 34-hour and 63-hour scale. The oscillation at the 63-hour scale is the strongest, so it is the first predominant period and the 34-hour scale is the second period.

4. Conclusions and discussion

The researches on the evolution patterns of fine particulate matter (PM2.5) will yield useful results for the haze prediction that is an important step to protecting people from the health damages caused by the poor air quality. Previous researchers used to utilize the overall temporal information to analyze the evolutionary features of PM2.5. However, it is hard to get the localized oscillation characteristics based on the global time series since the time series of PM2.5 concentration is nonstationary. The wavelet analysis is good at exploring the temporal structure of an energy spectrum at multiple scales and provides a continuous function of time and frequency.

To explore the evolutionary characteristics of PM2.5 concentration, we applied the Morlet wavelet transform to two distinct circumstances that one is based on the daily PM2.5 concentration data collected from six automatic monitoring stations in Chengdu ranging from June 2014 to June 2017 and the other is on the hourly PM2.5 concentration in 120 h when the haze is serious. The reason that we used the PM2.5 concentration both on the daily and hourly time scale is to provide the time-frequency properties at different temporal granularities, which will be very helpful for haze predictions at different time spans.

In the time-scale analysis of PM2.5 concentration in three years, there exist multiple oscillation periods in the scale of 14–32 d, 62–104 d, 105–178 d and 216–389 d. But compared with other periods, the oscillation on the 216–389-day scale is the strongest in the entire time domain. And the principal period of PM2.5 evolved continuously within the three years. It decreases with time. Specifically, In the first 400 days, the principle oscillation is around 325 d, and it shifts to about 300d after 500th d. According to the analysis of the wavelet variance, we found that the 298d is the first dominant period, which influences the global evolution, and the process has experienced three up-down conversions within the three years.

The oscillation amplitude of PM2.5 exhibits a trend of increase. In the first 500 days, the oscillation is relatively powerless, but the energy increases continuously and becomes stable after the 500th d.

While studying the time-scale features of PM2.5 concentration in the heavy-haze days, we collected the hourly PM2.5 concentration during 0:00 on 2nd January to 23:00 on January 6, 2016, in total amount of 120 h. The PM2.5 concentration is characterized by a strong 62-h oscillation during the first 20 h, and the predominant period suddenly changes from 62 h to 34 h at the 20th h and it lasts to the 80th h. After the 80th h, the principal period increases to 64 h gradually. According to the variance, we got a more accurate oscillation conditions that the 63 h is the first predominant period and the energy at this scale is strongest.

Although the temporal properties of the PM2.5 evolution show an apparently dominant oscillation, these relatively powerless periods still play a role in the time series. Especially in the hourly evolution, there is a 34-hour scale oscillation between the two 63-hour-scale oscillations. Therefore, considering the temporal characteristics on the multiple scales is reasonable and critical for the haze prediction. But the features shown in the analysis of the PM2.5 evolution still give little information about the reasons of the haze formation. The work on the joint analysis between the temporal characteristics of PM2.5 and the regional conditions, such as the geographical features of the place, remains.

Funding

Science & Technology Department of Sichuan Province Grant/Contract numbers: 2019YJ0189 Grant/Contract numbers: 2018SZDZX0013.

References

Abry, P., Veitch, D., 1998. Wavelet analysis of long-range-dependent traffic[J]. IEEE Trans. Inf. Theory 44 (1), 2–15.
Adrianac, F., Claudia, W.R., Cryan, S., et al., 2008. Wavelet analysis of wintertime and spring thaw CO_2 and N_2O fluxes from agricultural fields[J]. Agricultural & Forest Meteorology 148 (8), 1305–1317.
Baliunas, S., Frick, P., Sokoloff, D., et al., 1997. Time scales and trends in the central England temperature data (1659–1990): a wavelet analysis[J]. Geophys. Res. Lett. 24 (11), 1351–1354.
Chen, Y., Wang, S., Han, W., et al., 2017. A new air pollution source identification method based on remotely sensed aerosol and improved glowworm swarm optimization[J]. IEEE Journal of Selected Topics in Applied Earth Observations & Remote Sensing (99), 1–11.
Daubechies, I., 1990. The wavelet transform, time-frequency localization and signal analysis[J]. IEEE Trans. Inf. Theory 36 (5), 961–1005.
Dong, M., Kuang, Y., Kuang, Y., 2009. PM2.5 concentration prediction using hidden semi-Markov model-based times series data mining[J]. Expert Syst. Appl. 36 (5), 9046–9055.
Doyle, M., Dorling, S., 2002. Visibility trends in the UK 1950–1997[J]. Atmos. Environ. 36 (19), 3161–3172.
Farge, M., 1992. Wavelet transforms and their applications to turbulence[J]. Annu. Rev. Fluid Mech. 24 (1), 395–458.
Flandrin, P., 1992. Wavelet analysis and synthesis of fractional Brownian motion[J]. IEEE Trans. Inf. Theory 38 (2), 910–917.
Fuller, G.W., Carslaw, D.C., Lodge, H.W., 2002. An empirical approach for the prediction of daily mean PM 10, concentrations[J]. Atmos. Environ. 36 (9), 1431–1441.
Grinsted, A., Moore, J.C., 2004. Application of the cross wavelet transform and wavelet coherence to geophysical time series[J]. Nonlinear Process. Geophys. 11 (5/6), 561–566.
Gupta, A.K., Karar, K., Srivastava, A., 2007. Chemical mass balance source apportionment of PM10 and TSP in residential and industrial sites of an urban region of Kolkata, India.[J]. J. Hazard. Mater. 142 (1), 279–287.
Hu, S., Mcdonald, R., Martuzevicius, D., et al., 2006. UNMIX modeling of ambient PM2.5 near an interstate highway in Cincinnati, OH, USA[J]. Atmos. Environ. 40 (2), 378–395.
Hu, M., Jia, L., Wang, J., et al., 2013. Spatial and temporal characteristics of particulate matter in Beijing, China using the Empirical Mode Decomposition method[J]. Sci. Total Environ. 458, 70–80.
Jian, L., Zhao, Y., Zhu, Y.P., et al., 2012. An application of ARIMA model to predict submicron particle concentrations from meteorological factors at a busy roadside in Hangzhou, China[J]. Sci. Total Environ. 426 (2), 336–345.
Lonati, G., Butelli, G.P., Romele, L., et al., 2005. Major chemical components of PM2.5 in Milan (Italy)[J]. Atmos. Environ. 39 (10), 1925–1934.

Meyers, S.D., Kelly, B.G., O'Brien, J.J., 1993. An introduction to wavelet analysis in oceanography and meteorology: with application to the dispersion of Yanai waves[J]. Mon. Weather Rev. 121 (10), 2858–2866.
Morlet, J., Arens, G., Fourgeau, E., et al., 1982. Wave propagation and sampling theory—part I: complex signal and scattering in multilayered media[J]. Geophysics 47 (2), 203–221.
Neiburger, M., Wurtele, M.G., 1949. On the nature and size of particles in haze, fog, and stratus of the Los Angeles region[J]. Chem. Rev. 44 (2), 321–335.
Okamoto, S., Hayashi, M., Nakajima, M., et al., 1990. A factor analysis-multiple regression model for source apportionment of suspended particulate matter[J]. Atmospheric Environment.part A.general Topics 24 (8), 2089–2097.
Rodríguez, S., Querol, X., Alastuey, A., et al., 2003. Events affecting levels and seasonal evolution of airborne particulate matter concentrations in the Western Mediterranean[J]. Environmental science & technology 37 (2), 216–222.
Schichtel, B.A., Husar, R.B., Falke, S.R., et al., 2001. Haze trends over the United States, 1980–1995[J]. Atmos. Environ. 35 (30), 5205–5210.
Song, C., Pei, T., Yao, L., 2015. Analysis of the characteristics and evolution modes of PM2. 5 pollution episodes in Beijing, China during 2013[J]. Int. J. Environ. Res. Public Health 12 (2), 1099–1111.
Thurston, G.D., Ito, K., Lall, R., 2011. A source apportionment of U.S. fine particulate matter air pollution[J]. Atmos. Environ. 45 (24), 3924–3936.
Torrence, C., Compo, G.P., 1998. A practical guide to wavelet analysis[J]. Bull. Am. Meteorol. Soc. 79 (1), 61–78.
Vautard, R., Yiou, P., Van Oldenborgh, G.J., 2009. Decline of fog, mist and haze in Europe over the past 30 years[J]. Nat. Geosci. 2 (2), 115.
Wang, Y.S., Yao, L., Wang, L.L., et al., 2014. Mechanism for the formation of the January 2013 heavy haze pollution episode over central and eastern China[J]. Science China Earth Sciences 57 (1), 14–25.
Weng, H., Lau, K.M., 1994. Wavelets, period doubling, and time–frequency localization with application to organization of convection over the tropical western Pacific[J]. J. Atmos. Sci. 51 (17), 2523–2541.
Xi-Qin, A.O., Fei, J.L., Chen, J.L., et al., 2018. Analysis and prediction of PM2.5 based on multivariate statistics-taking Hefei area as an example[J]. Journal of Jiamusi University 36, 96–99.
Yin, H.L., Ye, Z.X., Yang, Y.C., Yuan, W., Qiu, C.Y., Yuan, H.W., Wang, M., Li, S.P., Zou, C. W., 2013. Evolution of chemical composition of fogwater in winter in Chengdu, China. J. Environ. Sci. 25, 1824–1832.
Zhang, Z., Zhang, X., Gong, D., et al., 2015. Evolution of surface O3 and PM2. 5 concentrations and their relationships with meteorological conditions over the last decade in Beijing[J]. Atmos. Environ. 108, 67–75.
Zheng, W., Li, X., Yin, L., et al., 2017. Wavelet analysis of the temporal-spatial distribution in the Eurasia seismic belt[J]. Int. J. Wavelets Multiresolution Inf. Process. 15 (03), 1750018.